WELDING RESEARCH

SUPPLEMENT TO THE *WELDING JOURNAL*, MAY 1993
Sponsored by the American Welding Society and the Welding Research Council

Microstructure and Mechanical Properties of Gas-Shielded Welding of C-Mn-Ni Steel

Different types of welding wires were tested to assess the effect on impact and tensile properties by welding out of position

BY D. J. ABSON

ABSTRACT. A range of semiautomatic gas-shielded arc welding consumables was selected in order to assess their suitability for producing uphill groove welds in 30-mm (1.2-in.) thick structural steel to BS4360:1986 Grade 50EE. In addition to a 1.2-mm (0.047-in.) diameter solid welding wire, 1.2-mm-diameter rutile and basic flux cored and metal cored welding wires were employed, all with Ar-20%CO_2 shielding. A 2-mm (0.08-in.) diameter self-shielded flux cored welding wire was also included. All deposits contained nominally 1% Ni. Constant voltage power sources were used for the rutile and self-shielded electrodes, and synergic pulsed power sources for the remainder. All welding was carried out without preheat, and with a maximum interpass temperature of 150°C (302°F).

For all except the self-shielded deposit, the as-deposited microstructure consisted predominantly of fine-grained acicular ferrite.

In both the as-welded and stress-relieved conditions, the strength of all welds exceeded the strength requirements of the base plate. Charpy toughness exceeded the plate toughness requirement (≥27 J at –50°C; 20 ft-lb at –58°F) for the deposits produced with both the solid welding wire and the basic flux cored wire, but not for the metal cored and the self-shielded deposits. The rutile flux cored wire deposit, which gave >27 J at –50°C as-welded, showed a shift in Charpy transition curve of ≥60°C (140°F) upon stress relieving for 1.2 h at 600°C (1112°F).

In crack tip opening displacement (CTOD) tests (on B X B specimens), the basic flux cored electrode deposits displayed upper shelf behavior down to –30°C (–22°F), both as-welded and stress-relieved. The rutile flux cored electrode deposit changed from upper shelf to lower shelf behavior at –10°C (14°F) upon stress relieving. The remaining deposits generally showed upper shelf behavior at 10°C (50°F) as-welded, and at –10°C stress-relieved, with the exception of the stress-relieved self-shielded deposit, which did not show fully ductile behavior at –10°C.

KEY WORDS

C-Mn-Ni Electrodes
Flux Cored Electrode
Metal Cored Electrode
Weld Metal
Microstructure
Mechanical Properties
Structural Steel
Deposit Composition
Semiautomatic Welds
Pulsed Welding

D. J. ABSON is with the Materials Dept., The Welding Institute, Abington Cambridge, U.K.

Paper presented at the AWS 71st Annual Convention, held April 22–27, 1990, in Anaheim, Calif.

Introduction

A wide variety of consumables, including shielded metal arc (SMA), self-shielded, and gas-shielded types, is available for the welding of C-Mn structural steels such as BS4360:1986 Grade 50EE (formerly 50E in BS4360:1979), which may be employed in hostile environments such as the North Sea. The composition and procedural variables influencing weld metal microstructure, and hence, mechanical properties are reasonably well understood for the submerged arc and SMA processes. Very much less information, however, has been published for continuous wire, semiautomatic welding. This work was therefore intended not only to produce quantitative mechanical property data, but also to examine the relationship between deposit composition and microstructure for this process.

Previously published work includes reviews of flux cored consumables available in 1970 (Ref. 1) and in 1980 (Ref. 2). Subsequent experimental work in-

Table 1 — Chemical Analysis (wt-%) of the 30-mm-Thick Base Plate (Coded 1A527), Compared with the Chemical Requirements of the Specification BS 4360: 1979 Grade 50E (BSC P11 Rev. 5) MOD, and of BS 4360: 1986 Grade 50EE

	Element, wt-%														
Identity	C	S	P	Si	Mn	Ni	Cr	Mo	V	Cu	Nb	Ti	Al	N	O
Plate[b]	0.11	0.003	0.016	0.33	1.39	0.02	0.02	<0.005	<0.002	0.02	0.036	<0.002	0.037	0.0064	0.0011
Specification	≤0.16	≤0.012	≤0.025	0.10-0.45	1.10-1.50	≤0.2	≤0.2	≤0.08	≤0.02	≤0.2	≤0.04	—	≤0.05[a]	≤0.010	
Grade 50EE	≤0.18	≤0.030	≤0.040	0.10-0.50	≤1.50	—	—	—	0.003-0.10	—	0.003-0.08	—	—	—	—

(a) Soluble Al.
(b) Sn, Co, As, Pb, Zr, <0.005; B, Ca <0.0003. TWI analyses S/86/317 and O/N 86/148.
Note: Plate mechanical property requirements: Yield strength >345 MPa, tensile strength = 490-640 MPa, for 16-40 mm thickness, absorbed Charpy energy >27J at −50°C.

cluded studies on welds produced in the flat and vertical positions using a number of solid, metal cored and flux cored welding wires (Refs. 3–5). Both mild and C-Mn steels to BS4360 Grades 43A and 50D were employed, but many of the consumables in these earlier investigations are not appropriate for the welding of BS4360 Grade 50EE, which has a more stringent Charpy toughness requirement of ≥27J at –50°C (20 ft-lb at –58°F). Moreover, there was generally little comment on the microstructures produced.

For the present study, a variety of welding consumables was chosen which contained nominally 1% Ni to improve low-temperature toughness and which, according to the manufacturers' all-weld-metal data, gave Charpy toughness exceeding that specified for the base steel employed, viz. >27 J at –50°C. Each consumable was assumed to be broadly representative of that type of welding wire. While short-circuiting transfer can be employed for out-of-position welding with solid, metal cored and basic flux cored welding wires, synergic pulsed welding was used in order to achieve improved operability. This process, which was first described by Amin and coworkers (Ref. 7), is well established for welding with solid welding wires, where it either permits or facilitates out-of-position welding (Refs. 8–12). It has also been reported to allow closer control of metal transfer, and to give improved penetration (Refs. 8,10) and weld toughness (Ref. 8). Extension of the process for use with metal cored and flux cored welding wires has been discussed (Refs. 8, 12). Both satisfactory (Refs. 13, 14) and generally unsatisfactory (Ref. 15) synergic pulsed welding has been reported with both types of consumable. Therefore, metal cored and basic flux cored welding wires were included in the present study in part to examine the feasibility of synergic operation.

Vertical uphill welding was selected as being representative of out-of-position welding, with the expectation that weld nitrogen levels might be higher than would occur for other positions. The weld metals were examined in the as-welded and stress-relieved conditions. Chemical analysis and metallographic examination were carried out, with assessment of deposit tensile and toughness properties, the last involving Charpy and CTOD testing.

Experimental Details

Materials

The plate employed was a 30-mm (1.2-in.) thick C-Mn-Si-Al-Nb steel, with a minimum yield strength of 345 MPa (50 ksi), which conformed to BS4360: 1986 Grade 50EE — Table 1.

The 1% Ni welding wires used in this study were a rutile (Ti-B) flux cored wire, a basic flux cored wire, a metal-cored wire and a solid wire, all of 1.2-mm (0.047-in.) diameter. A 2-mm (0.078-in.) diameter self-shielded flux cored wire was also used. The chemical compositions and the AWS designations for these electrode wires are given in Table 2. The analyses were obtained on remelted samples using a direct-reading optical emission vacuum spectrometer. In view of the presence of slag-forming elements, the analyses for the cored welding wires should be considered as semi-quantitative. Oxygen and nitrogen contents of the solid welding wire were determined by inert gas fusion in a Leco T-136 analyzer. Shielding gas, which was employed with all except the self-shielded wire, was Ar-20%CO_2, with a flow rate of 15 L/min (7 ft3/h).

Welding Details

Of the various ways in which comparisons could be made between the chosen consumables, it was decided that all the welds should be deposited in a similar sequence of beads, with the intention of producing welds all of which had a similar macroscopic appearance. An asymmetric double-V-groove preparation was employed (Fig. 1) in which the major side was welded first. This configuration permitted sampling of the potentially lower as-welded toughness root region (Ref. 3) not only in Charpy toughness tests, but also within the region of highest constraint (toward the

Table 2 — Chemical Analyses (wt-%) of Remelted Samples of the Wires Used in This Investigation

			Element, wt-%													
Wire Code	Wire Type	AWS Code[a]	C	S	P	Si	Mn	Ni	Cr	Mo	V	Cu	Ti	Al	B	N	O
1	Self-shielded flux cored	E71T8-K6	0.09	<0.002	0.005	0.23	0.80	0.83	0.16	0.02	<0.002	0.01	0.072	0.80	<0.0003	—	—
2	Rutile flux cored	E81T1-Ni1	0.05	0.011	0.015	0.47	1.56	1.08	0.04	0.005	0.03	0.02	0.087	0.005	0.0093	—	—
3	Metal cored	E70T-1	0.09	0.011	0.010	0.61	1.64	0.71	0.02	0.01	0.01	0.01	0.004	<0.003	<0.0004	—	—
4	Solid	—	0.10	0.004	0.006	0.69	1.30	1.38	0.05	0.005	0.002	0.05	0.102	0.012	<0.0003	0.009	0.009
5	Basic flux cored	E80T5-G	0.11	0.012	0.008	0.37	1.43	1.11	0.03	0.005	<0.002	0.06	0.011	0.016	<0.0003	—	—

Note: Nb < 0.002, except wire number 2, 0.022.
Sn, As < 0.005, except wire number 2, 0.01 Sn.
Co ≤ 0.005, except wire number 2, 0.01 and wire number 4, 0.04.
(a) AWS Specification A5.29-80, *Specification for Low Alloy Steel Electrodes for Flux Cored Arc Welding*. The manufacturer of the solid wire did not give an AWS designation.
TWI analyses S/86/406 and O/N 86/176.

Table 3 — Welding Parameters

Weld Code	Wire Type	Polarity	Pass Number	Mean Current, A	Mean Voltage, V	Travel Speed, mm/min	Wire Feed Speed, m/min	Pulse Parameters: High Pulse Current A	High Pulse Voltage, V	High Pulse Time, ms	Low Pulse Current, A	Low Pulse Voltage, V	Low Pulse Time, ms	Pulse Frequency, Hz	Arc Energy, kJ/mm	Mean Arc Energy, kJ/mm	Total Arc Time, min	Average Deposition Rate, kg/h
F	Self-shielded	−ve	1	191	16.9	70	1.8								2.7	2.9	137	2.0
			2	209	17.8	66	2.1								3.3			
			3	209	17.9	58	2.1								3.8			
			4[b]	200	17.3	77	1.9								2.6			
			5[b]	197	17.2	78	1.9								2.6			
			6[a]	209	17.7	75	2.1								2.9			
			7[a]	204	17.2	89	1.9								2.3			
R	Rutile flux cored	+ve	1	174	21.2	153	5.8								1.5	2.1	79	3.4
			2	193	22.1	146	6.7								1.8			
			3	200	23.0	99	6.8								2.8			
			4	204	23.5	95	7.0								2.9			
			5[b]	195	22.5	110	6.4								2.4			
			6[a]	204	22.9	143	6.7								1.9			
			7[a]	174	20.6	153	5.1								1.4			
M	Metal cored	+ve	1	54	28.2	85	3.0	340	37	1.3	20	27	10.8	83	1.3	2.2	122	2.2
			2	92	29.3	59	4.7	360	38	1.7	25	27	6.8	118	3.3			
			3	88	29.2	56	4.7	360	38	1.6	25	27	6.9	118	3.4			
			4[b]	87	28.8	66	3.6	380	37	1.8	20	27	7.8	104	2.8			
			5[a]	90	28.6	174	4.2	380	36	1.6	30	27	7.75	107	1.0			
			6[a]	88	28.6	101	4.0	400	37	1.6	25	27	7.8	106	1.8			
			7[a]	79	28.4	97	3.2	350	36	1.7	25	27	8.6	97	1.6			
S	Solid	+ve	1	68	27.4	77	2.9	340	36	1.6	20	26	9.0	94	1.8	2.4	130	2.1
			2	98	30.0	52	3.5	400	36	1.8	25	28	7.6	108	3.9			
			3	103	29.5	63	3.6	410	36	1.8	25	28	7.0	113	3.4			
			4[b]	78	28.1	68	3.4	395	35	1.4	25	27	8.3	103	2.3			
			5[a]	99	29.7	142	3.6	400	37	1.7	30	28	7.5	109	1.4			
			6[a]	94	30.5	82	3.6	360	37	1.9	30	29	7.9	102	2.4			
			7[a]	78	27.3	91	3.1	390	35	1.6	25	26	9.5	90	1.7			
B	Basic flux cored	+ve	1	101	23.8	113	4.5	375	33	1.7	50	22	9.2	92	2.2	3.0	112	2.4
			2	120	24.3	89	5.0	390	33	1.8	50	22	6.9	115	4.1			
			3	137	25.0	77	5.2	395	34	1.9	50	22	5.6	133	4.0			
			4	137	25.0	78	5.2	395	34	1.9	50	22	5.6	133	3.7			
			5[b]	126	24.7	81	4.7	380	34	1.8	50	22	6.0	128	1.6			
			6[a]	131	24.5	99	4.9	390	33	1.9	50	22	6.0	126	2.9			
			7[a]	115	24.2	81	4.6	380	33	1.9	50	22	7.85	103	2.2			

(a) Passes deposited in the second (minor) side.
(b) Cap on the first (major) side (split weave for Weld F).
1. The values of arc energy for the Synergic pulsed welding are only approximate, as they were calculated assuming an idealized square waveform, *i.e.*, the times required to reach the peak and the background current and voltage were assumed to be part of the peak time and the background time, respectively.
2. Values of electrode extension were 12-19 mm for Weld F and 12-15 mm for Weld B.
3. The flow rate for the Ar-20% CO_2 shielding gas (Welds R to L) was 15 L/min.
4. The wires were all 1.2 mm diameter, except the self-shielded wire, which was 2.0 mm.

center of the specimen) in CTOD test specimens, which were notched through the thickness.

The overall panel size for each weld was 1.4 X 0.25 m (4.6 X 0.81 ft). Restraint was provided by four strong-backs, each 50 mm (2 in.) thick, 250 mm (10 in.) wide and at least 150 mm (6 in.) deep, attached to the plate on the minor side, approximately equally spaced, and separated by restraining bars, which were welded between the strong-backs to counter bowing of the panel — Fig. 1. The panels were welded uphill without preheat, and with a maximum interpass temperature of 150°C (302°F). The major side of the preparation was filled completely before the strong-backs were removed. In order that any potentially lower toughness region in the root could be examined and tested, back-gouging was not employed. Instead, the root was lightly ground back to sound metal, and the second side of the weld was completed.

Both the rutile flux cored and the self-shielded flux cored welding wires welded satisfactorily with constant voltage power sources. Thyristor-controlled transformer/rectifier GMA welding power sources, a Lincoln Idealarc R35-400 and a Hobart Mega-MIG 450RVS were employed for the self-shielded and rutile flux cored consumable respectively, and an inverter preprogrammed synergic pulsed GMA welding power source (Fronius 500) was employed for the metal-cored and the solid welding wires. As this last machine did not have a suitable program for welding with the basic flux cored wire, a programmable synergic pulsed GMA transformer/ rectifier welding power source (AWP M450) was employed. The maximum current capability of the welding power sources was 400 A and 450 A respectively, for the constant voltage machines and 350 A (maximum mean current at 100% duty cycle) for the synergic power sources.

The pulse parameters employed for the synergic pulsed welding were those which gave the most stable arc. During welding, values of the parameters employed (Table 3) were read from traces produced on a Medelec oscillographic recorder. The welding parameters used with the constant voltage power sources were recorded with a portable arc monitoring device (PAMS II) (Ref. 16). The (mean) current and other welding details were within the ranges recommended by the consumable manufacturers, but were not necessarily the optimum values, as an attempt was made to employ a similar arc energy for corresponding beads in each of the welds, in order to facilitate comparison of the various consumable types. The travel speeds quoted in Table 3 were obtained by dividing the panel length by the arc time for each pass. Average deposition rates for each completed weld were evaluated using weld areas, determined

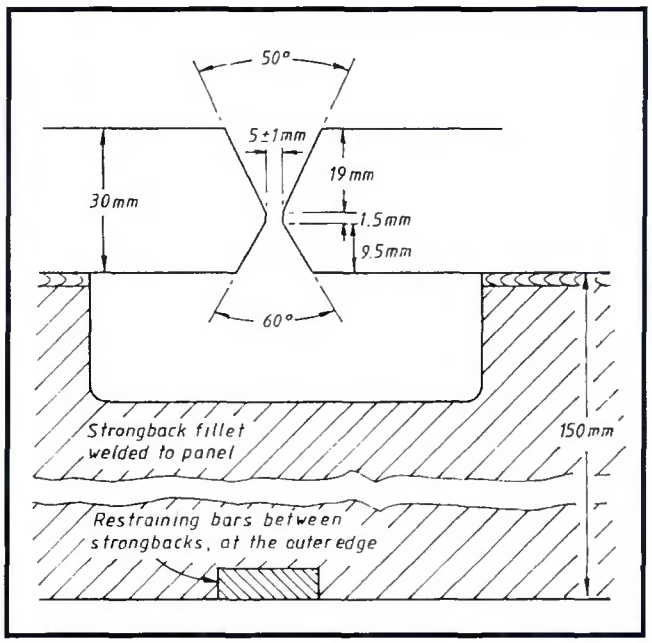

Fig. 1 — Weld preparation.

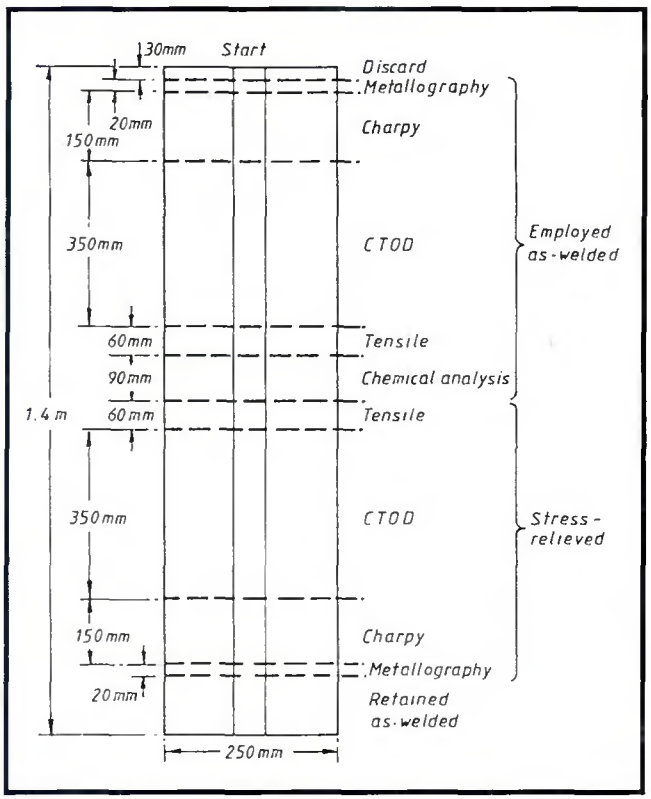

Fig. 2 — Cutting scheme.

from the macrosections, and total arc times.

Chemical Analyses of Weld Metals

The first pass root and second pass fill regions, corresponding approximately to the regions sampled by mechanical test specimens discussed below, were analyzed in an optical emission vacuum spectrometer, sparking directly onto the face of a longitudinal section down the weld central plane. For both the as-welded and stress-relieved portions of the panel, an estimate of the free nitrogen content was obtained, for each region, by difference between the total nitrogen content and the residual nitrogen after nitrogen extraction at 450°C for 1h in a hydrogen atmosphere. Samples for oxygen and nitrogen analyses were cut from each of the two regions and were again analyzed in a Leco TC-136 analyzer.

Determination of Mechanical Properties

After completion of welding, part of the panel was given a stress relief heat treatment at 600°C (1112°F) for 1.2 h, following the requirements of BS5500:1985, for example. The panels were sectioned as shown in Fig. 2.

In both the as-welded and stress-relieved conditions, sample extraction and testing are described below.

One longitudinal tensile specimen was extracted from the first pass root region, and one from the second pass fill region of each weld. These were BS18 specimens with a gauge length of 22.7 mm (0.9 in.) and a gauge diameter of 5.64 mm (0.22 in.). The tensile specimens and the blanks for the CTOD specimens discussed below were given a hydrogen release treatment of 40 h at 150°C, prior to testing, in order to simulate the escape of hydrogen in a fabrication prior to service. The tensile specimens were tested at room temperature.

Weld metal hardness was measured on transverse sections, using a Vickers diamond pyramid indenter and a 10-kg (22-lb) load.

From each of 10 transverse slices of each weld, two Charpy specimens were extracted, sampling approxi- mately the second pass fill and the first pass root regions. The specimens were notched through the thickness on the weld central plane, and each set was tested over a range of temperatures to provide a transition curve.

Nine square section (B X B) crack tip opening displacement (CTOD) specimens were extracted from each panel. They were notched through the thickness with a crack depth-to-specimen thickness (a/W) ratio of –0.25. They were tested in triplicate at temperatures within the range –50° to 30°C (–58° to 86°F). The fatigue precracking, the CTOD testing, and computation of the results were all carried out according to BS 5762:1979 (which is similar to the U.S. Standard E 1290-1989). Those specimens which did not break during the test were broken open after being chilled in liquid nitrogen. In order to induce the formation of a fatigue precrack with a straight front, the as-welded specimens were each locally precompressed by 1% (Ref. 17) prior to fatigue precracking. Testing was carried out in three-point bending under displacement control, at a crosshead displacement rate of 0.01 mm/s.

Metallographic and Fractographic Studies

Transverse sections of the weld, in both the as-welded and stress-relieved conditions, were ground and polished to a 1-μm diamond finish and were then etched in nital, prior to metallographic examination. Measurements were made of the percentages of as-deposited and reheated, *i.e.*, re-austenitized, regions on the weld central plane of the as-deposited specimens, in locations corresponding approximately to those sampled by the Charpy specimens. In addition, the percentages of the various microstructural constituents in the as-deposited microstructure, generally in the final pass on the second side, were assessed by counting an array of 1000 points, with the aid of a Swift point

counter. The terminology employed is that of Ref. 18.

Selected CTOD test specimens, which had fractured during testing, were subjected to detailed fractographic examination in a scanning electron microscope (SEM). The approximate point of initiation of the unstable fracture was marked with a small paint spot on the fracture surface, and each specimen was sectioned through this point perpendicular to the fracture surface (to give a transverse weld section), thereby allowing metallographic examination of the microstructure in the initiation region (Ref. 19).

Results

Welding Behavior

The data in Table 3 show that all welds were completed in a total of seven passes. Generally, one bead per layer was employed. However, there were some unintentional variations in both the sequence of beads and the arc energies of beads in particular locations. The differences are a consequence of differences in welding behavior of the various consumables and the difficulty of maintaining a particular value of arc energy. Overall, the arc energies were greater for the self-shielded flux cored and the basic flux cored welding wires, and the variation in arc energy was greater for the synergic pulsed welding than for the constant voltage power sources. The fierce arc and deep penetration of the self-shielded electrode, and the use of slightly higher levels of arc

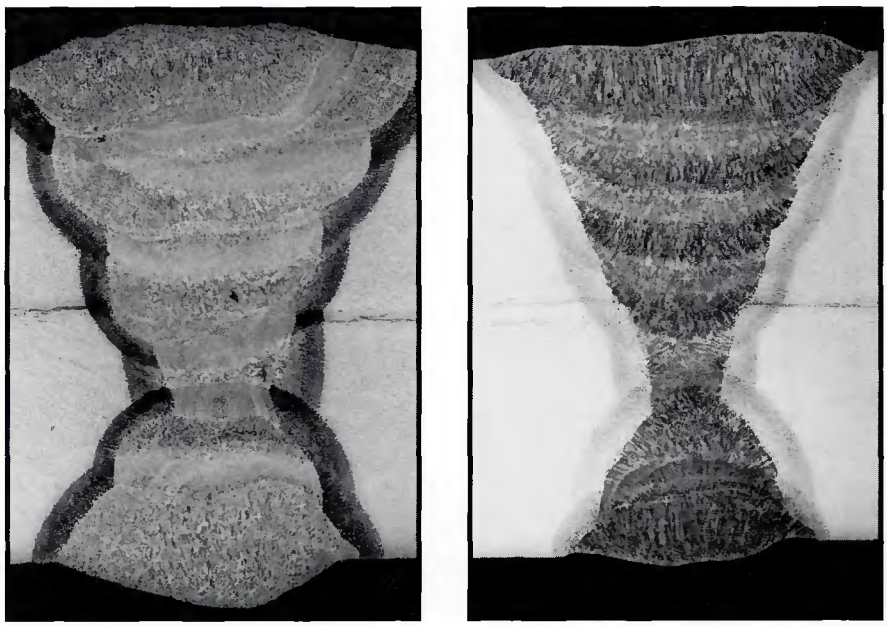

Fig. 3 — Macrographs of selected welds in the as-welded condition, showing the bead profiles. Left — Weld F; right — Weld R.

Table 4 — Chemical Analyses (wt-%) of the Welds, IIW CE and Estimated Inclusion Volume Fractions I[(a)]

Weld Code	Wire Type	Element, wt-% C	S	P	Si	Mn	Ni	Cr	Mo	V	Cu	Nb	Ti	Al	B	O	Total N	Free N AW	Free N SR	IIW CE	I[(a)]
F root	Self-shielded flux cored	0.08	0.002	0.009	0.26	1.02	0.55	0.11	0.01	0.002	0.02	0.012	0.038	0.61	<0.0003	0.011	0.020	0.0000	0.0007	0.31	0.06
F cap	Self-shielded flux cored	0.07	0.002	0.008	0.24	0.94	0.67	0.13	0.01	0.002	0.01	0.007	0.045	0.68	<0.0003	0.011	0.029	0.0016	0.0004	0.30	0.06
R root	Rutile flux cored	0.08	0.010	0.015	0.41	1.39	0.85	0.03	<0.005	0.02	0.02	0.021	0.068	0.014	0.0064	0.058	0.006	0.0009	0.0002	0.38	0.36
R cap	Rutile flux cored	0.07	0.010	0.015	0.37	1.39	0.89	0.03	<0.005	0.02	0.02	0.019	0.065	0.011	0.0069	0.057	0.005	0.0016	0.0003	0.37	0.36
M root	Metal cored	0.07	0.011	0.011	0.50	1.43	0.72	0.02	0.005	0.01	0.01	0.003	0.008	0.007	0.0003	0.095	0.010	0.0049	0.0012	0.36	0.65
M cap	Metal cored	0.07	0.011	0.010	0.46	1.33	0.74	0.02	0.005	0.01	0.01	0.002	0.007	0.006	<0.0003	0.088	0.004	0.0013	0.0004	0.35	0.61
S root	Solid	0.10	0.005	0.008	0.51	1.06	1.23	0.04	0.005	0.005	0.05	0.005	0.033	0.007	<0.0003	0.032	0.011	0.0044	0.0011	0.37	0.20
S cap	Solid	0.10	0.005	0.007	0.54	1.08	1.32	0.04	0.005	0.002	0.05	<0.002	0.037	0.006	<0.0003	0.035	0.015	0.0059	0.0008	0.38	0.22
B root	Basic flux cored	0.09	0.014	0.009	0.27	1.21	0.98	0.02	<0.005	<0.002	0.06	0.005	0.004	0.017	<0.0003	0.042	0.010	0.0041	0.0015	0.37	0.31
B cap	Basic flux cored	0.09	0.015	0.009	0.26	1.24	1.04	0.02	0.005	<0.002	0.06	0.003	0.004	0.013	<0.0003	0.045	0.010	0.0050	0.0017	0.38	0.34

Note: Sn ⩽ 0.005, except Weld R cap, 0.01.
Co ⩽ 0.01, except Weld S root, 0.03 and Weld S cap, 0.04.
As ⩽ 0.005.
Ca, Pb, Zr all < 0.005, except Weld F (root and cap), Zr = 0.03.
TWI analyses S/86/402, O/N 86/174 and O/N 88/10.
IIW CE = C+Mn/6 + (Cr + Mo + V)/5 + (Ni + Cu)/15.
(a) The estimated inclusion volume fraction, I, was calculated according to the method employed in Ref. 20. This procedure ignored the contribution from AlN, which contributes an estimated additional 0.14% in the root and 0.19% in the cap for Weld F.

Table 5A — Percentages of As-Deposited Regions on the Weld Central Plane

Weld Code	Wire Type	Region Sampled[a]	% As-Deposited
F	Self-shielded flux cored	Root	54
		Fill	60
R	Rutile flux cored	Root	50
		Fill	52
M	Metal cored	Root	71
		Fill	52
S	Solid	Root	73
		Fill	57
B	Basic flux cored	Root	44
		Fill	48

(a) Root = region corresponding to that sampled by the Charpy toughness specimens extracted from the first side root region. Fill = region corresponding to that sampled by the Charpy toughness specimens extracted from the second side.

5B — Percentages of Microstructural Constituents in the As-Deposited Microstructure, Counted at a Magnification of 500

Weld Code	Wire Type	Region Sampled[b]	PF[a], %	FS(A)[a], %	AF[a], %
F	Self-shielded flux cored	Cap	8	48	44
F	Self-shielded flux cored	Root	3	74	22
R	Rutile flux cored	Cap	0	12	88
M	Metal cored	Cap	7	13	80
S	Solid	Cap	5	10	85
B	Basic flux cored	Cap	6	15	79

(a) PF = primary ferrite; FS(A) = ferrite with aligned second phase; AF = acicular ferrite.
(b) Cap = capping pass on the second side.
Root = first side root, second pass.
Note that, for Weld F, in both the cap and the root, the distinction between PF(G) and PF(I) could not be made. For the remaining welds, PF is entirely PF(G).

energy, resulted in the deposition of larger beads for weld F than for any of the others. The arc energy of the root pass of this weld was higher than that in any of the other welds, and the capping pass on the first side, (an area sampled only toward the outer edge of the CTOD specimens and not in any of the other mechanical test specimens) was completed with a split weave. The major side of welds F, R and B was completed in five passes, compared with four passes for welds M and S. Macrographs of selected welds are presented in Fig. 3.

The synergic pulsed power source used for welds M and S gave spray transfer, easy control of the weld pool, low spatter, and a reasonably good bead surface appearance. In spite of adjustment of the synergic pulse parameters to give the most stable arc condition for the basic flux cored welding wire (Weld B), the welder reported that the weld pool was difficult to control. The globular transfer achieved with this consumable gave rise to high spatter, a coarse ripple on the bead surface, and the presence of some entrapped slag.

Welds F and R were deposited by globular and by spray transfer, respectively, using the constant voltage power sources. For both the self-shielded and the rutile flux cored electrodes, the weld pool was easy to control and there was little spatter. The self-shielded welding wire gave a coarse ripple on the bead surface. By contrast, the rutile flux cored electrode gave a particularly smooth bead profile. The average deposition rate for this consumable was substantially larger and the total arc time was correspondingly shorter than for any of the others — Table 3.

Weld Chemical Analyses

Chemical analyses (Table 4) show that there were only minor differences in C content, but rather larger differences in the levels of Si, Mn, Ni, Ti, Al, B, N and O. In all cases except in the root of the self-shielded deposit, the free nitrogen content was reduced substantially by stress relieving. Weld F contained a small amount of Cr (~0.1%), which is presumably a deliberate addition. Small but significant amounts of Ti were present in all welds. However, the Ti contents of Welds M and B were much lower than in Welds F and S, and also in Weld R, which contained a significant level (~0.0065%) of boron; Weld R also had the lowest total nitrogen content and low estimated free nitrogen levels, possibly because of the presence of Ti and boron. In spite of having the highest total nitrogen content, Weld F had very low estimated free nitrogen levels (presumably due to the presence of ~0.65%Al and ~0.04%Ti), and also a very low oxygen content (~0.01%), which may also be a consequence of the high Al level. The low oxygen and sulfur contents of this weld resulted in a very low estimated inclusion content, comparable with those found in gas tungsten arc welds. By contrast, Weld M contained almost an order of magnitude more oxygen, presumably because of the use of a small amount of slag formers and very low levels of Al or other strong deoxidants. In contrast to all the other welds, this deposit had a somewhat higher nitrogen content in the root region than in the cap pass, possibly resulting from incomplete gas shielding and the slightly higher high-pulse arc voltage in the early passes.

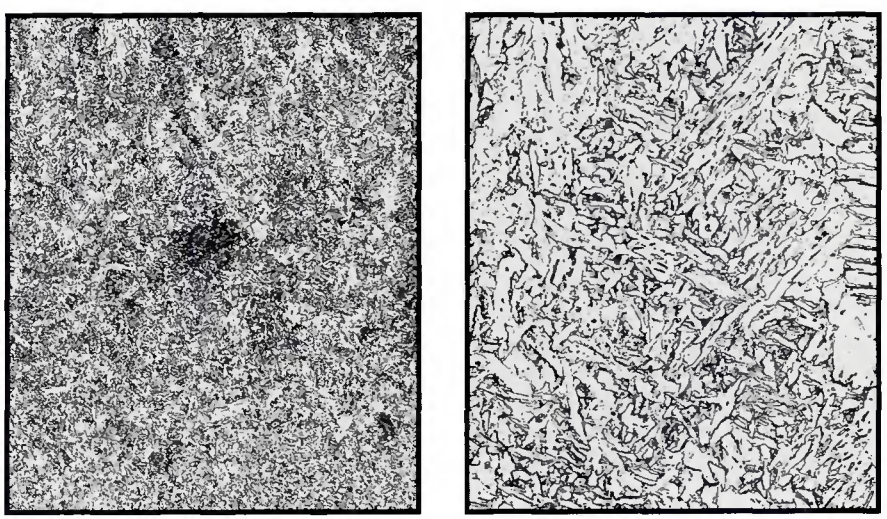

Fig. 4 — Microstructure of second-side weld metal of Weld F, as-welded. A — As-deposited region of the cap and underlying re-austenitized region, 50X; B — as-deposited region of the cap, 500X.

Microstructural Studies

Macrographs illustrating representative weld transverse sections are shown in Fig. 3. The percentages of as-deposited weld metal in the regions corresponding to those sampled by the Charpy specimens were determined as discussed previously. The results are shown in Table 5A. The highest percentages (~70%) occur in the first side root region in Welds M and S. These figures

are undoubtedly influenced strongly by the presence of a low arc energy bead in the first pass of the second side of these welds. The remaining values range from 44 to 54% in the first side root and from 48 to 60% in the second side fill region.

The percentages of the various microstructural constituents in the as-deposited microstructure are shown in Table 5B. As-deposited microstructures were closely similar in the cap and root region of each weld, except for Weld F. Hence, it was only for this weld that the root region was also assessed. Micrographs of second side weld metal in selected as-welded specimens are presented in Figs. 4 and 5. The low inclusion volume fraction of Weld F (~0.05%, compared with 0.20 to 0.65% for the other welds) probably provided insufficient nucleants to produce a fine acicular ferrite microstructure — Fig. 4 and Table 5B. The microstructure contained comparatively large colonies of FS(A), which would be expected to have an adverse effect on cleavage resistance. The as-deposited microstructure of Weld M (Fig. 5) and also of Welds S and B, contained a high proportion of fine-grained acicular ferrite, with sufficient grain-boundary nucleated transformation products to reveal the location of the prior austenite boundaries. By contrast, Weld R, the rutile flux cored deposit, had such a uniform fine-grained microstructure that it was difficult to identify the prior-austenite grain boundaries, and thus at high magnification, it was difficult to locate the boundaries between as-deposited and reheated weld metal. (The 12% ferrite with aligned second phase, FS(A), in this deposit was present in small regions among the acicular ferrite laths.)

The effect of stress-relieving, in all deposits, was to induce precipitation at many of the ferrite grain boundaries — Fig. 6.

Tensile and Hardness Results

The tensile and hardness data are presented in Table 6. In the as-welded condition, the yield strength, tensile strength and hardness of Weld F are the lowest, reflecting the low IIW CE of this weld — Table 4. The highest strength and hardness were obtained in Weld R, probably as a consequence of the moderately high levels of Si, Mn, Ti and B, and also the presence of ~0.02%Nb. As noted earlier, this weld also had a fine and very uniform microstructure, which would have contributed to its strength and to a high value (0.9) of the yield-to-tensile ratio. Of the remaining welds, Weld S had the highest strength, to which the presence of ~0.03%Ti probably made some contribution. Values of the elongation generally lay in the range of 15 to 20%, with 62 to 74% reduction of area.

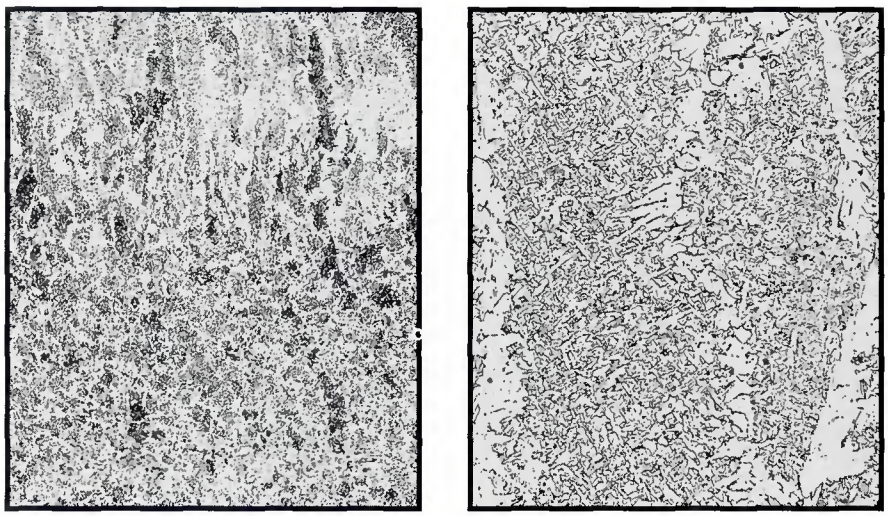

Fig. 5 — Microstructure of second-side weld metal of Weld M, as-welded. A — As-deposited region of the cap, and underlying re-austenitized region, 50X; B — as-deposited region of the cap, 50X.

In the stress-relieved condition, yield strength values range from ~480 to 680 MPa (~69.6–98.6 ksi), and the tensile strength values range from ~590 to 743 MPa (85.6–107.7 ksi). In both cases, the highest value is associated with the fill region of Weld R. Stress relieving was expected to reduce the tensile strength of all welds, in view of the hardness changes, which are discussed below. The reductions in tensile strength were ~20 to ~40 MPa (2.9–5.8 ksi) in the fill regions of Welds F, R and S, but were substantially larger in the fill regions of Welds M and B, namely 59 and 54 MPa (8.5 and 7.8 ksi), respectively — Table 6. The tensile strength changes in the root were rather more complex. Stress relieving generally reduced the tensile strength, but it even produced a small increase in tensile strength in the root region of Weld F, and there was a much more substantial increase in strength in the root region of Weld S (41 MPa; 5.9 ksi).

The changes in yield strength followed a broadly similar pattern to those of the tensile strength, including an increase (by 28 MPa; 4.1 ksi) in the root region of Weld S. Exceptions were in the root region of Welds F and B, and in the fill region of Weld M, Table 6. Elongation and reduction in area were essentially unchanged by stress-relieving —

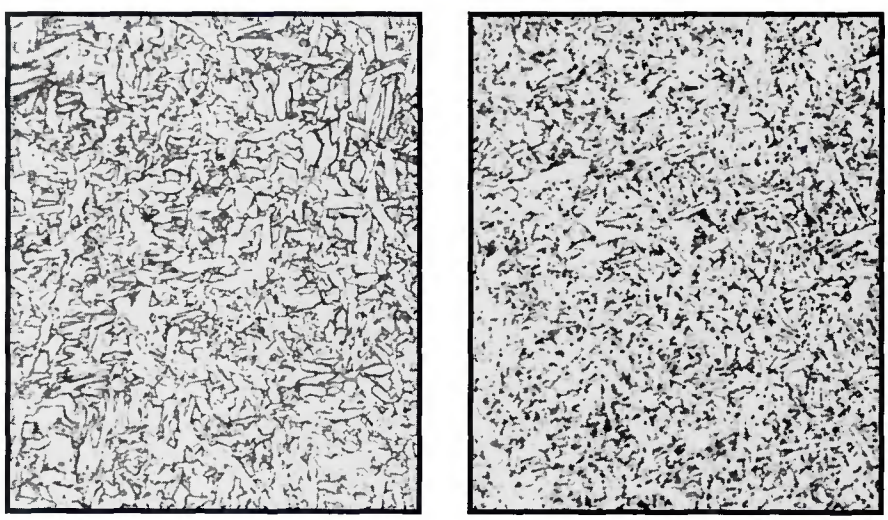

Fig. 6 — Micrographs of as-deposited weld metal in the capping pass on the second (minor) side of Weld S. A — As-welded; B — stress-relieved.

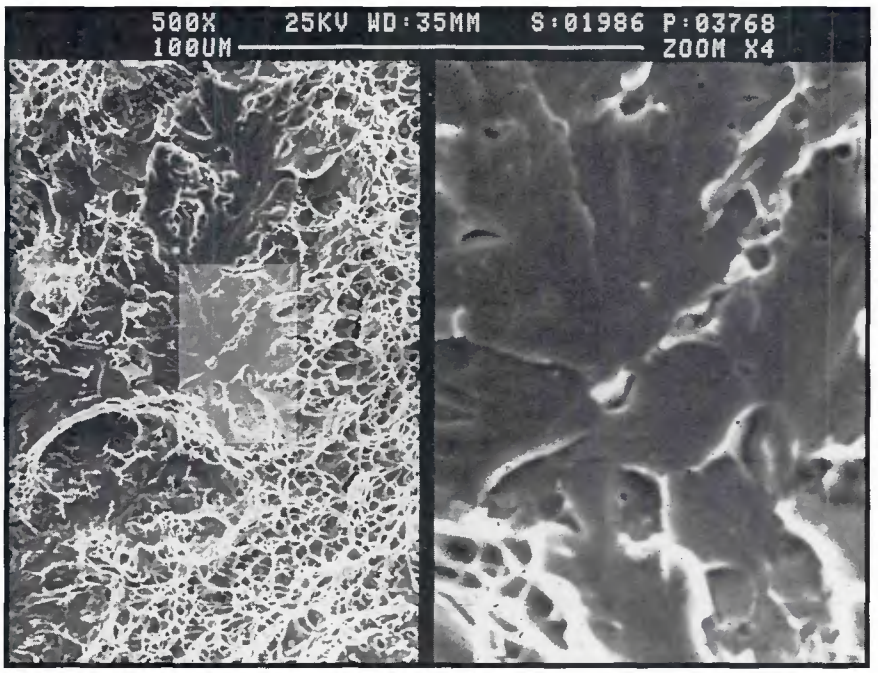

Fig. 7 — Fractograph from within a region of cleavage fracture on as-welded CTOD Specimen M-3 (dc = 0.12 mm at –10°C) showing local initiation of cleavage fracture at a small region of microphase, ~500X/~2000X.

Table 6. Thus, in spite of the removal of strain damage, ductility has not been improved.

In the as-welded condition, the mean hardness ranged from 200 HV10 in the root of weld F to 271 HV10 in the fill region of Weld R. In all deposits, the fill region was harder than the root, although the difference was minimal in the case of Weld M — Table 6.

After a stress relief heat treatment, the mean hardness values generally ranged from ~190 HV10 to ~215 HV10, the exceptions being Welds R and S. The changes in hardness produced by stress-relieving are also shown in Table 6. Compared with the as-welded values, these mean hardness values are ~10 HV10 lower for Welds F and B and 13 to 19 HV10 lower for the remainder, except for the fill region of Weld R and the root region of Weld M, where the hardness changes upon stress relieving were –24 and –31 HV10, respectively.

Charpy Toughness

With the exception of the root region of Weld F, the as-welded Charpy toughness was higher than the minimum toughness specified for the plate of 27 J at –50°C — Table 7. The highest upper shelf Charpy toughness was found in Weld F, consistent (Ref. 21) with its low calculated inclusion volume fraction — Table 4. The toughness transition for the root region of this specimen is particularly steep, falling from >140 J at –20°C to <20 J at –60°C (>103 ft-lb at –4°F to 14.7 ft-lb at –76°F). The low inclusion volume fraction also undoubtedly makes a contribution to the steepness of the transition curve, as reported by Bailey and Pargeter (Ref. 20). Conversely, Weld M, with a high inclusion content, displayed a comparatively low upper shelf Charpy toughness, and a shallower slope of the Charpy transition curve compared

Table 6 — As-Welded and Stress-Relieved Tensile and Hardness Data

		As-Welded Data						Stress-Relieved Data						Change in Tensile Properties and in Mean Hardness on Stress-Relieving				
Identity	Electrode Wire Type	Yield Strength, MPa	Tensile Strength, MPa	Yield Tensile Ratio	Elong-ation, %	Reduct-ion of Area, %	Hardness min-max / mean HV10	Yield Strength, MPa	Tensile Strength, MPa	Yield Tensile Ratio	Elong-ation, %	Reduct-ion of Area, %	Hardness min-max / mean HV10	Yield Strength, MPa	Tensile Strength, MPa	Elong-ation, %	Reduct-ion of Area, %	Hardness min-max / mean HV10
F Root	Self-shielded flux cored	532	605	0.88	19	69	185-225 / 200	503[a]	612[a]	0.82	14	60	177-220 / 189	–29	+7	–5	–9	–11
F Fill	Self shielded flux cored	528[a]	615	0.86	20	74	199-212 / 207	484[a]	596	0.81	19	72	191-203 / 197	–44	–19	–1	–2	–10
F Root	Rutile flux cored	676[a]	736	0.92	17	64	226-274 / 244	616	690	0.89	19	60	206-248 / 231	–60	–46	–2	–4	–13
F Fill	Rutile flux cored	706	781	0.90	15	62	249-292 / 271	680	743	0.92	17	67	238-253 / 247	–26	–38	–2	+5	–24
M Root	Metal cored	532	626	0.85	18	64	195-237 / 218	514[a]	609	0.84	21	64	170-205 / 187	–18	–17	+3	0	–31
M Fill	Metal cored	575[a]	655	0.88	12[b]	47[b]	209-227 / 220	490[a]	596	0.82	20	66	178-217 / 201	–85	–59	[b](AW)	[b](AW)	–19
S Root	Solid	585[a]	652	0.90	17[b]	7[b]	217-240 / 230	613[a]	693	0.88	17	67	195-230 / 216	+28	+41	[b](AW)	[b](AW)	–14
S Fill	Solid	665[a]	743	0.90	19	68	249-264 / 256	618[a]	702	0.88	19	67	218-263 / 237	–47	–41	0	–1	–19
B Root	Basic flux cored	584[a]	645	0.90	19	65	195-233 / 212	527	620	0.85	20	68	190-213 / 201	–57	–25	+1	+3	–11
B Fill	Basic flux cored	544[a]	653	0.83	19	68	207-251 / 224	502[a]	599	0.84	20	69	190-228 / 214	–42	–54	+1	+1	–10

(a) 0.2% proof strength.
(b) Defect on fracture surface.

with the other welds.

The Charpy impact results for the stress-relieved welds are also summarized in Table 7, with the changes in temperature for 27, 40 and 100 J (20, 30 and 74 ft-lb), compared with the as-welded condition also included. The most dramatic consequences of stress relieving are shifts in the Charpy curves of ~60°C (108°F) for the root region and >100°C (180°F) in the fill region of Weld R. Stress relieving was also detrimental to toughness for the fill region in Weld F. For the three remaining welds, M, S and B, it changed from being detrimental at 27 J (shifts of 20°, 14° and 2°C, respectively) to beneficial at 100 J (shifts of –22°, –16° and again –16°C, respectively).

Concerning toughness in the root region, similar behavior was observed for Weld M, where a stress relief heat treatment increased the temperature for 27 J by 13°C (23°F) and decreased the temperature for 100 J by 6°C (11°F). The remaining welds behaved differently. A stress relief heat treatment became deleterious to toughness in the root for Welds F and S as the toughness criterion changed from 27 J (a shift of –14°C and

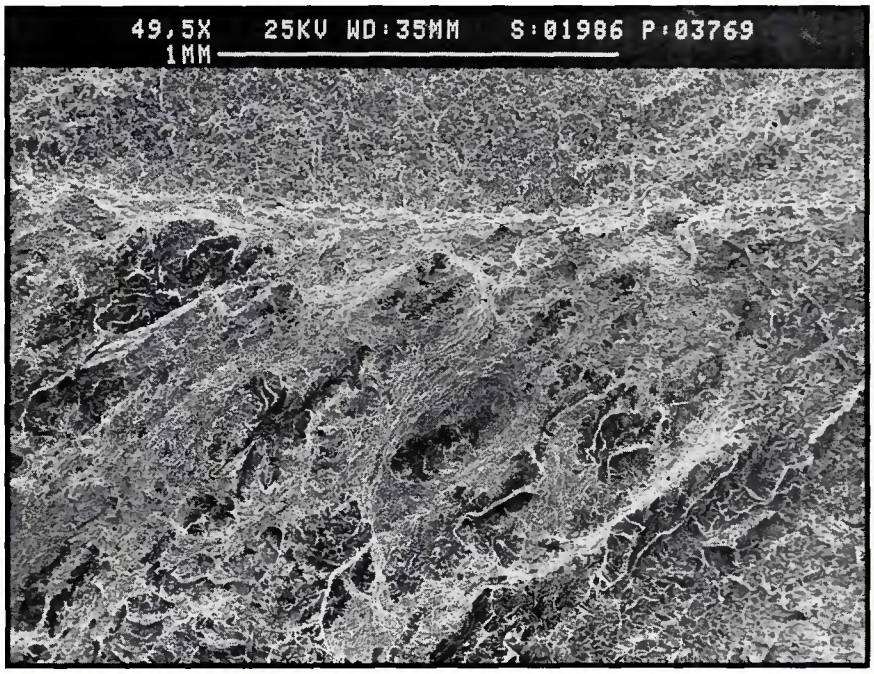

Fig. 8 — Fractograph showing a high density of regions of cleavage fracture on as-welded CTOD Specimen M-3, 50X.

Table 7 — As-welded and Stress-Relieved Toughness

		Charpy Toughness From Transition Curves										Change in Charpy Temperature on Stress-Relieving, °C			Critical CTOD for Bx8 Specimens Notched through the Thickness, mm							
		As-Welded Data					Stress-Relieved Data								As-Welded				Stress-Relieved			
	Electrode Wire	Temperature, °C			Energy, J		Temperature, °C			Energy, J												
Identity	Type	27J	40J	100J	-20°C	-40°C	27J	40J	100J	-20°C	-40°C	27J	40J	100J	−50°C	−30°C	−10°C	+10°C	−50°C	−30°C	−10°	+10°C	+30°C
F Root	Self-shielded flux cored	−40	−38	−34	142	28	−54	−42	−8	74	44	−14	−4	+26	—	0.072[a]	0.75[b]	1.61[a]	0.79[b]	0.60[b]	1.45[b]	—	—
																0.052[c]	0.43[b]	1.59[a]	0.15[c]	0.58[b]	1.30[bp]	—	—
F Fill	Self-shielded flux cored	−64	−52	−14	90	54	−40	−28	−12	49	28	+24	+24	+26	—	0.030[c]	0.31[b]	1.14[a]	0.037[c]	0.059[c]	0.59[b]	—	—
R Root	Rutile flux cored	−76	−64	−26	112	74	−12	4	32	24	18	+64	+68	+58	0.34[b]	1.70[a]	1.85[a]	—	—	—	(0.029[c]	0.31[cp]	0.93[bp]
															0.15[b]	1.56[a]	1.25[a]	—	—	—	(0.024[cd])	0.036[cp]	0.048[cp]
R Fill	Rutile flux cored	−72	−66	−22	101	85	32	45	97	13	10	+104	+111	+119	0.15[b]	0.39[b]	1.01[a]	—	—	—	0.021[cd]	0.012[cp]	0.046[cp]
M Root	Metal cored	−58	−40	42	55	40	−45	−31	36	50	32	+13	+9	−6	—	0.43[b]	0.46[b]	1.05[a]	0.28[b]	0.63[b]	2.06[a]	—	—
															—	0.39[b]	0.39[b]	0.39[b]	0.26[b]	0.57[bd]	1.68[a]	—	—
M Fill	Metal cored	−64	−46	28	62	46	−44	−34	6	64	33	+20	+12	−22	—	0.072[c]	0.12[c]	0.97[a]	0.039[c]	0.51[cp]	1.67[a]	—	—
S Root	Solid	−68	−56	−20	102	63	−68	−48	−2	66	46	0	+8	+18	0.27[b]	0.87[b]	1.68[a]	—	0.59[b]	1.25[b]	3.78[a]	—	—
															0.13[b]	0.78[b]	1.67[a]	—	0.45[b]	0.59[b]	2.53[a]	—	—
S Fill	Solid	−80	−62	−4	79	57	−66	−44	−20	100	47	+14	+18	−16	0.10[b]	0.46[b]	1.26[b]	—	0.41[b]	0.29[c]	2.14[a]	—	—
B Root	Basic flux cored	−62	−48	2	70	46	−74	−56	−28	110	52	−12	−8	−30	0.51[b]	1.05[a]	1.45[a]	—	1.48[b]	1.80[a]	2.24[a]	—	—
															0.38[b]	1.03[a]	1.03[a]	—	1.31[a]	1.77[a]	2.02[a]	—	—
B Fill	Basic flux cored	−70	−56	12	73	55	−68	−54	−4	80	55	+2	+2	−16	0.25[b]	0.83[a]	0.78[a]	—	1.03[a]	1.24[ad]	1.97[ad]	—	—

(a) δ_m = critical CTOD at first attainment of maximum force plateau (or test stopped).
(b) δ_u = critical CTOD, after slow crack growth, at either, 1) unstable fracture, or 2) onset of arrested brittle crack or pop-in.
(c) δ_c = critical CTOD, in the absence of any slow crack growth, at either 1) unstable fracture, or 2) onset of arrested brittle crack or pop-in.
— Not determined.
( ) Invalid test result.
[p]Pop-in.
(d) Defect on fracture surface.

Table 8 — Metallographic and Other Information Relating to Sectioned As-Welded CTOD Specimens

Weld Code	Specimen Number	Wire Type	Critical CTOD, mm	Test Temperature, °C	Distance from Major Side Plate Surface, mm	Distance From Base of Second Side, mm	Initiation Bead	Microstructural Region[a]
F	7	Self-shielded flux cored	$\delta_c = 0.052$	−30	14.0	7.5	Second pass	GC
F	8	Self-shielded flux cored	$\delta_c = 0.030$[b]	−30	19.3	2.5	Root pass	AD
R	8	Rutile flux cored	$\delta_c = 0.15$	−50	17.0	3.0	Root pass	Probably GC
M	7	Metal cored	$\delta_c = 0.072$	−30	10.5	8.0	Second pass	GR/IC
S	8	Solid	$\delta_u = 0.10$	−50	10.5	7.5	Second pass	IC
B	7	Basic	$\delta_u = 0.38$	−50	7.8	12.5	Third pass	SCRH

Note: 1. In all specimens which were examined, initiation of cleavage fracture occurred in first side weld metal.
2. In weld R, the different microstructural regions were not well-defined, as a consequence of the uniformity of the transformation structure
(a) GC = grain-coarsened reheated; AD = as-deposited; GR = grain-refined reheated; IC = intercritical; SCRH = subcritically reheated.
(b) Pop-in.

no change, respectively) to 100 J (shifts of 26° and 18°C, respectively). By contrast, stress relief was always beneficial in the root region for Weld B.

As a stress relief heat treatment generally produced a reduction in strength, it might be expected that Charpy toughness would be reduced at the higher toughness levels (where failure occurred predominantly by microvoid coalescence) and increased at the lower toughness levels (where failure occurred predominantly by cleavage). Such toughness changes were, in fact, only observed in the root region of Weld F; however, the converse was not observed in the root region of Weld S, where a stress relief heat treatment raised the strength. In many instances, stress relieving increased the slope of the Charpy toughness curve, as observed for multiple-pass submerged arc welds by Bailey and Pargeter (Ref. 22).

Crack Tip Opening Displacement Results

The critical CTOD data are presented in Table 7. Considering first the as-welded CTOD data, it will be noted that the test temperature range was varied to suit the toughness of each weld. The highest toughness at −50°C was observed for Weld B (basic flux cored deposit). This weld showed fully ductile behavior at both −10° and −30°C. Similar levels of toughness were achieved in Welds R and S. For Weld R, the beneficial effect of a fine and uniform microstructure was probably partially offset by the comparatively high strength of this deposit, and also by its moderately high inclusion content. The reason for the slightly poorer toughness of Weld S compared with B is not clear. Both have similar strengths, at least in the root region, and similar levels of free nitrogen. Weld S has a substantially greater percentage of as-deposited weld metal in the root region (Table 5A), and this is suggested as a possible explanation, although the results considered in the next section do not show that as-deposited regions are necessarily the lowest toughness regions in these two deposits.

Toughness was lower for Welds F and M, where upper shelf behavior was not observed until 10°C. For Weld F, it is clear that the adverse effect on toughness of a coarse microstructure has overridden the potentially beneficial influences of comparatively low strength and a low inclusion content. Conversely, for Weld M the detrimental effect of the high inclusion content was probably overriding. However, although large inclusions are known to be capable of initiating cleavage fracture (Refs. 23–27), inclusions were not clearly seen to be responsible for the initiation of fracture at the primary initiation sites in the present welds.

The critical CTOD results for the stress-relieved condition are also presented in Table 7, where it may be seen that all welds were tested at temperatures of −50°, −30° and −10°C, except for Weld R, where the first three specimens were tested at −10°C, with subsequent specimens being tested at 10° and 30°C. Once again, a marked deleterious effect of stress relieving on the toughness of Weld R is readily apparent. For all other welds, toughness improved upon stress relief heat treatment, and Weld B displayed upper shelf behavior over the whole of the test temperature range. Welds M and S showed slightly lower toughness than Weld B, with Weld M showing one very low toughness value (0.039 mm) at −50°C. The greatest scatter (in log critical CTOD) was observed for Welds F and R. The former showed a reasonable level of toughness at −10°C (lowest value 0.59 mm), but even at 30°C the toughness of Weld R was very low (lowest value 0.046 mm).

The strong deleterious effect of a stress relief heat treatment on critical CTOD for Weld R is, as noted previously, attributable to the occurrence of intergranular fracture. For Welds F and B, the improvements in critical CTOD resulting from stress relief are attributable to an improvement in cleavage resistance in the root region, as indicated by the Charpy toughness data for these two welds. For Welds M and S, such an explanation does not apply. The observed behavior is particularly puzzling for Weld M, where the critical CTOD improved substantially, but Charpy toughness decreased in the root.

Metallurgical Studies of Selected CTOD Specimens

In the as-welded condition, the specimens selected for fractographic and metallographic study were generally the lowest toughness specimen from each weld — Table 8. These included specimen F-8 ($\delta_c = 0.30$ mm), for which an audible click during testing had indicated the occurrence of a "pop-in"; however, no corresponding arrested cleavage fracture could be discerned on the fracture surface. Small welding discontinuities appeared on the fracture surfaces of mechanical test specimens for all welds, but were rare for Welds F, M and S. Slag defects were noted in the root region on the fracture faces of a few CTOD samples from Welds R and M, and on most specimens from Weld B.

Fractographic examination in the binocular microscope was employed to reveal the location of the point of fracture initiation. With some difficulty, approximate locations of the probable fracture initiation sites were found and marked. Examination of the metallographic sections through these regions permitted establishment of their location in the weld — Table 8. It will be noted that, in these as-welded specimens, fracture always initiated in the first (major) side, generally in the first or second pass, within the central 10 mm of the 30-mm-thick specimen. An exception to this was specimen B-7, where fracture initiation occurred in the third bead of the first side, at a distance of only ~8 mm from the level of the plate surface, indicating that no regions with a lower cleavage resistance were sampled in the central one-third of the specimen.

Occasional instances of local initiation of cleavage fracture at inclusions (~1-μm diameter) were observed, as reported by several investigators (Refs. 23–27).

However, unlike the samples of some of these investigators, the phenomenon was not a general one, and did not appear to have played a major role in the initiation of unstable fracture, as such features were not always seen in the general region in which fracture appeared to have initiated. In some instances, (local) cleavage fracture initiation appeared to have occurred at microphases (Fig. 7) as observed by Terlinde, *et al.* (Ref. 26) and by Chen and Yan (Ref. 28).

The metallographic observations reported in Table 8 include the microstructural regions in which fracture appeared to have initiated. In the majority of welds, initiation occurred in re-austenitized or partially re-austenitized regions, implying that for all the consumables it would not necessarily be beneficial to toughness to deposit shallower layers, thereby reducing the percentage of as-deposited weld metal.

On the fracture surfaces of the (as-welded) specimens from Weld M, isolated patches of cleavage fracture were observed within the band of ductile tearing below the fatigue precrack. Only one or two such features, which were up to ~300 μm long and up to ~200 μm wide, occurred on the specimens which had given δ_m CTOD values, whereas several such features occurred on specimens which had given δ_u values. A particularly high incidence occurred in specimen M-3 (δ_c = 0.12 mm), within a band of mixed mode fracture beside the main cleavage fracture initiation region — Fig. 8. Clearly, none of the features observed was sufficient to initiate unstable fracture under the prevailing test conditions. However, it is considered probable that the occurrence of slightly larger low toughness features, or the chance occurrence of two such regions immediately adjacent, or a lowering of the test temperature, would allow them to do so. Such features have been reported previously (Refs. 28,29) and have been suggested as contributing to scatter in CTOD values, attributable to variations in their number density and their distance from the fatigue crack tip.

In the light of the marked adverse effect of a stress relief heat treatment on the toughness of Weld R, selected stress-relieved toughness test specimens from this weld were subjected to a detailed fractographic examination. Study of the fractured Charpy specimens revealed that the principal fracture mode, over the whole temperature range studied, in the columnar (as-deposited) regions was intergranular fracture, with respect to the prior austenite grains. Such fracture also occurred in coarse-grained reheated regions, particularly in the later passes on each side. The intergranular surfaces were linked by occasional bands of quasi-cleavage toward the bottom end of the temperature range studied and by microvoid coalescence toward the top end of the range. The transition between these two nodes of linkage of intergranular fracture occurred at ~–20°C — Fig. 9.

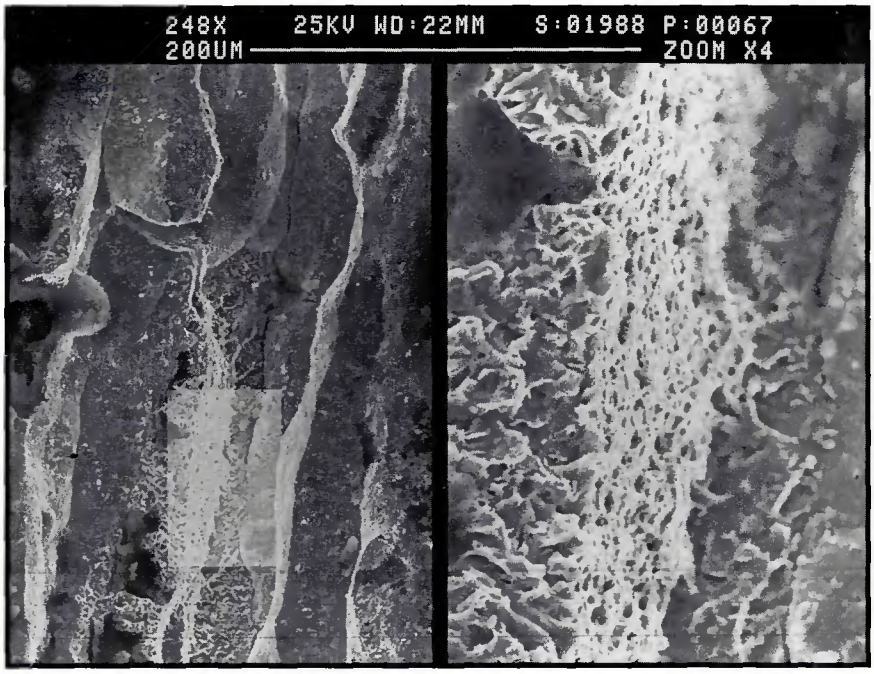

Fig. 9 — Fractograph showing intergranular fracture linked by both quasi-cleavage and microvoid coalescence in as-deposited weld metal in the fill region of the Weld R stress-relieved Charpy specimen tested at –20°C. ~250X/~1000X.

In the grain-refined regions, fracture occurred by cleavage or quasi-cleavage at the lower end of the temperature range, with linkage of patches of such fracture occurring by microvoid coalescence at intermediate temperatures — Fig. 10. Towards the top of the temperature range studied, failure of the grain-refined regions occurred almost entirely by microvoid coalescence.

Fractographic examination in the SEM of tested stress-relieved CTOD specimens from Weld R also revealed that the predominant fracture mode in the columnar (as-deposited) and grain-coarsened reheated regions was intergranular fracture. Intergranular fracture occurred so readily that it was commonly observed within the fatigue precrack regions. In spite of the apparent ease with which intergranular fracture occurred in this weld, fracture initiation, as indicated by river markings, generally occurred in re-austenitized regions.

Examination of Charpy specimens from Weld S (which had similar toughness to Weld R in the as-welded condition, and which also contained a substantial level of Ti (~0.035%) revealed that the low temperature fracture mechanism was cleavage. Moreover, only occasional large elongated cleavage facets, indicating the location of the as-deposited regions, were observed in these specimens.

Discussion

Welding Behavior

This investigation has demonstrated that out-of-position semiautomatic welding with small (1.2-mm) diameter metal cored, basic flux cored and solid welding wires can be achieved using synergic pulsed power sources. The present pulse frequency vs. wire feed speed values fall within the scatter-band of data presented by Ma and Apps (Ref. 11) for one drop per pulse in synergic pulsed welding with solid electrode wires. Except for the presence of entrapped slag in the root in some welds, notably in Weld B, welding behavior was satisfactory, and it can be expected that such entrapped slag would have been removed if backgouging had been employed.

With the rutile flux cored welding wire, a stable arc, smooth metal trans-

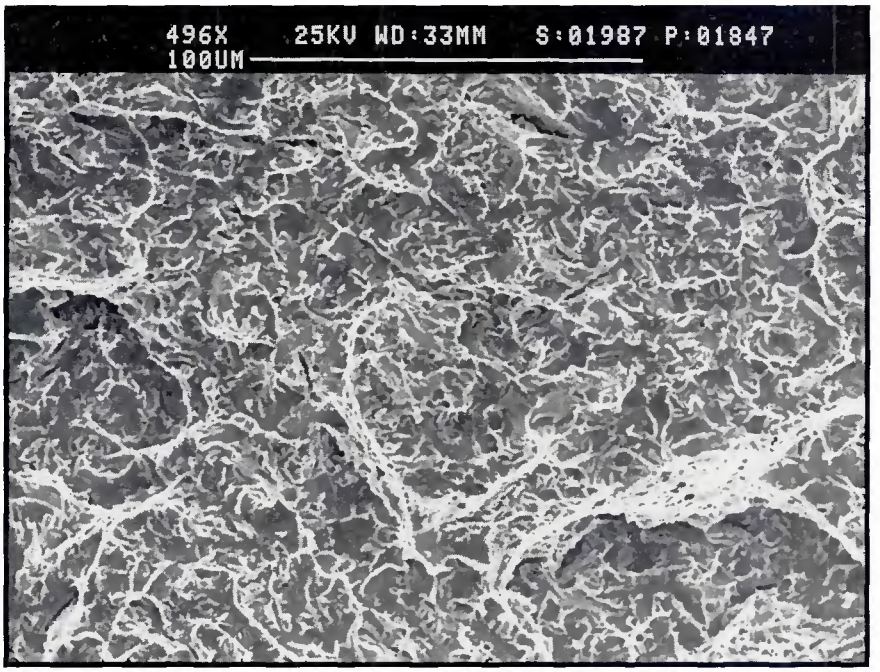

Fig. 10 — Quasi-cleavage linked by microvoid coalescence in a re-austenitized region of the specimen shown in the previous figure. ~1000X.

fer, low spatter and very smooth bead appearance were obtained using a constant voltage power source. The high melt-off rate achieved with this wire permitted the use of faster travel speeds, resulting in a substantially shorter total arc time than for the other consumables.

Lower levels of as-welded Charpy and CTOD toughness were obtained with a 2-mm-diameter C-Mn-Ni self-shielded welding wire than with the other consumables, and thus back-gouging, or an alternative welding procedure to that employed in the present study, may well be necessary to give welds with adequate toughness for this consumable. However, the consumable has the considerable advantage, particularly for on-site applications, of not requiring a shielding gas.

Strength and Hardness

With the exception of the root regions of Welds F and S, a stress relief heat treatment reduced deposit strength, and in all cases it reduced deposit hardness. The strength reduction was substantial (>40 MPa; 6 ksi) in the fill region of three of the welds, namely Welds M, S and B — Table 6. The observed behavior presents a very complex picture, which cannot be explained in detail. It is to be expected that the stress relief heat treatment would produce softening by dislocation recovery, and that this would lower the yield strength more than the tensile strength. The cause of the strength increases (for the tensile strength of the root region of Weld F and for the yield and tensile strength of the root region of Weld S) has not been studied in detail, but is presumed to be intragranular precipitation inhibiting dislocation motion. This precipitation, of nitrides or carbonitrides, reduced the free nitrogen content of all welds — Table 4. It should be noted that, in spite of the reduction in strength in most of the welds, they all still exceeded the strength requirements for BS4360:1986 50EE plate — Table 6.

Weld Metal Toughness

Viewed overall, the as-welded Charpy and CTOD toughness levels achieved were reasonably high, with the possible exception of the root of Weld F, which was the only region failing to meet the Charpy toughness required for the plate, *viz.* >27 J at –50°C. From Table 7, the relative ranking of the various welds depends on the criterion applied, but, in terms of CTOD cleavage resistance, Weld B (made using a basic flux cored electrode) has the highest as-welded low-temperature toughness, with the self-shielded Weld F being lowest. The toughness values obtained will depend on the arc energy employed; however, the present arc energies were selected as representative of fabrication practice, and on this basis the data are considered to be broadly typical of the various consumables, although optimum toughness levels have probably not been achieved.

Clearly, the most marked toughness changes which occurred on stress relief heat treatment were the reduction in toughness in Weld R, where the Charpy transition curve was displaced to higher temperatures by –60°C in the root region and by >100°C in the fill region, and where the critical CTOD changed from upper shelf to lower shelf behavior at –10°C. Such behavior is more extreme than, but is generally in line with, experience in industry; however, the phenomenon is not widely publicized. The toughness changes were associated with a change in the low-temperature mode of failure to predominantly intergranular fracture, in both as-deposited weld metal and in grain-coarsened reheated regions. This behavior is attributable to the prior austenite boundaries being preserved during transformation, rather than being lined with (soft) ferrite. These boundaries are then potential sites for the segregation and precipitation of boron and phosphorus (Table 4), which have an embrittling effect. It is therefore considered unlikely that the high level of Ti in this deposit is solely responsible for the observed behavior. Somewhat similar Charpy toughness behavior has been reported previously, where an as-deposited submerged arc weld gave intergranular fracture between –40°C and 30°C (Ref. 30). The submerged arc welds were deposited using a basic flux with a Mn-Mo-Ti-B welding wire and a high Al plate microalloyed with substantial additions of both Nb and V; thus, the resulting weld composition was broadly similar to that of Weld R. It is notable that similar behavior was reported not to have occurred in a related weld containing lower levels of Al and V. For the basic flux cored weld, the small change in Charpy toughness resulting from stress relief heat treatment, particularly for the second side fill region, is consistent with results obtained for all weld metal deposits of similar composition, produced with basic-coated SMA electrodes (Ref. 31). In Weld F, the most likely explanation for the slightly lower toughness in the root compared with the fill region is concluded to stem from the differences in microstructure — Table 5B. Noting that the compositional differences between root and fill regions are generally small, the small variations in the heat sink and in arc energy and bead shape between the first side root and second side fill passes may have contributed to the development of the observed microstructures in Weld F.

For the remaining welds, the CTOD was improved by a stress relief heat treatment, and the changes in Charpy toughness were not especially significant in Welds F, S and B. The selection of a double-V-groove preparation, and the use

of only light backgrinding in the root, permitted the sampling of the potentially low toughness root region in both Charpy toughness tests and in CTOD tests in which specimens were notched through the thickness on the weld central plane. In view of the small difference in as-welded toughness between the root and fill regions and, for Weld S, the higher strength of the latter, it appears that, with the possible exception of Weld F, strain age damage was minimal for all welds. Certainly, the level of restraint should have been sufficient to ensure that any toughness degradation due to strain aging or to straining alone would be minimal[1], and the similar strength of these two regions for Weld F supports this view. The enhanced cleavage initiation resistance caused by stress relief heat treatment may well be due not only to some reduction in yield strength, but possibly also to a reduced effect of free nitrogen. Certainly, the free nitrogen contents in both root and fill regions were decreased considerably by the heat treatment.

The CTOD results (Table 7) typically show δ_m values at the highest test temperature and δ_u values at the next lower test temperature, 20°C (36°F) lower. (An exception to this is Weld B, which gave δ_m critical CTOD values at both –10° and –30°C.) For many applications, the levels of toughness obtained in the present welds therefore generally indicate suitability for service at least at –10°C, and at even lower temperatures for some of the consumables.

Critical CTOD values depend not only on test specimen size and shape, but also on crack length. For example, Anderson (Ref. 32) observed a shift of ~6°C (11°F) in CTOD transition curve associated with a change in the ratio of crack depth to specimen width (a/W) from ~0.2 to ~0.52. Both Towers and Garwood (Ref. 33) and Tweed and Knott (Ref. 24) observed a decrease in δ_m with increasing a/W. Thus, the present results allow comparisons between the various welds in this study, but care is needed in attempting to make comparisons with the results of other investigations in which the specimens may be of different size or configuration.

The scatter obtained in the CTOD results is worthy of comment. With the notable exception of Welds F and R in the stress-relieved condition, critical CTOD values vary by a maximum factor[2] of 7 (in Weld M), with a more usual factor of ~2.5. This may be linked to the difficulty of locating the primary cleavage initiation site during fractographic examination. It is probable that there were generally several potential fracture initiation sites within the process zone ahead of the (advancing) crack tip in each CTOD specimen, and that the fracture initiation in one such region triggered cleavage fracture in several other regions nearby, making it impossible to establish by fractographic examination which of these had failed first. Thus, it appears that, so far as cleavage resistance is concerned, there were no major microstructural inhomogeneities giving rise to regions of toughness significantly below that of surrounding material. As noted above, Welds F and R, in the stress-relieved condition, showed much greater scatter in CTOD values (factors of ≤~21 for Weld F and ≤~26 for Weld R). This observation suggests that stress-relieving actually produced microstructural inhomogeneities in these two deposits.

Implications of the Present Findings

On the basis of the observed welding behavior and weld metal mechanical properties obtained, all the consumables examined are clearly of potential application for steel fabrications where semiautomatic welding offers advantages from the productivity viewpoint. The successful use of synergic pulsed welding will be noted, and application of the method in practice should be examined further. In any fabrication program, procedure test welds would be deposited using one or more selected consumables and processes. Compared with SMA electrodes, the consumables used in the present study have the advantage of a higher duty cycle, and they allow the flexibility of either semiautomatic or fully automatic operation. The welds that formed the basis of the present study were chosen as being broadly representative of different types of consumables which, on the basis of the information supplied by the manufacturers, were expected to give mechanical properties exceeding those specified for BS4360:1986 Grade 50EE plate (Table 1). In the as-welded condition, only the self-shielded flux cored deposit, Weld F, failed to meet these Charpy toughness criteria, and it also failed to do so after stress relief heat treatment. Thus, the process advantages for this consumable must be traded against the weld toughness. The rutile flux cored welding wire performed well, not only in giving acceptable mechanical properties, but also in allowing deposition of weld metal at a rate which was substantially greater than that achieved with the other consumables. However, the toughness falls to an unacceptably low level after a stress relief heat treatment. As current codes require postweld heat treatment for joints in heavier section sizes, consideration should be given to restricting the use of this type of consumable to fabrications where a stress relief heat treatment will not be carried out. This will generally imply joints with plate thicknesses ≤50mm.

In spite of the substantial improvement in critical CTOD upon stress relieving the weld deposited with the metal cored welding wire (with the lowest temperature at which upper shelf behavior occurred being shifted from 10° to –10°C), the reduction in Charpy toughness was sufficient enough that this weld failed to meet the plate toughness criterion of ≥27 J at –50°C. Thus, use of this type of consumable too may be restricted to fabrications that are not to be subjected to a stress relief heat treatment.

The welds produced with the basic flux cored welding wire gave the highest toughness in both the as-welded and stress-relieved conditions, and the Ti-containing solid welding wire also performed well, giving only slightly lower toughness. Considering both the as-welded and stress-relieved data, only these two consumables produced welds that met the toughness criterion specified for the plate, namely ≥27 J at –50°C. This suggests that these two consumables might be favored for butt joint welding thick-section material that is to be given a PWHT.

This study has explored some of the criteria on which selection of consumables would be made, including deposition rate and resulting weld strength and toughness, not only in the as-welded condition, but also after a stress relief heat treatment, where few data are available for GMA welds. The investigation has shown that root toughness was not substantially lower than that in the fill region, even without the back-gouging, which would generally be carried out when using these consumables, in order to avoid root defects. Thus, the several consumable types merit consideration for semiautomatic (or even fully automatic) out-of-position welding of BS4360:1986 Grade 50EE and similar steels.

With the exception of Weld F, the deposits examined displayed predominantly acicular ferrite microstructures, and this has doubtless contributed to the generally good toughness obtained, although the propensity for initiation of CTOD fracture in reheated regions must be recognized. The general relationships

1. It will be noted that the temperature employed for the hydrogen release treatment did not exceed the maximum interpass temperature, and thus should not have produced further strain age damage.

2. This is a ratio of the highest to the lowest critical CTOD value at a particular temperature.

between composition and microstructure, and hence toughness, have been well explored for the submerged arc process and in large part the present results seem consistent with available information. However, substantially more study is necessary to define the factors controlling deposit microstructure, especially in terms of the role of minor elements, notably Al.

Conclusions

A series of uphill welds has been produced in 30-mm-thick steel plate which met the requirements of BS4360:1986 Grade 50EE steel plate, using a range of C-Mn-Ni (nominally 1% Ni) welding wires. Argon-20% CO_2 shielding was employed for all except a self-shielded flux cored electrode. Constant voltage power sources were employed for this consumable and for a rutile flux cored electrode, while synergic pulsed power sources were employed for a metal cored, a basic flux cored and a solid consumable. The as-welded and stress-relieved mechanical properties and microstructure of these welds has been investigated, and the following conclusions drawn:

1) Stable welding conditions were achieved by synergic pulsed welding with the metal cored and the solid consumables, and to a lesser extent the basic flux cored welding wire. However, the welds produced with the basic flux cored electrode and, to a lesser extent, the rutile flux cored electrode contained entrapped slag in the root, indicating a need for back-gouging. The highest deposition rate (shortest total arc time) was achieved with the rutile flux cored consumable, deposited with a constant voltage power source.

2) As-deposited microstructures consisted predominantly of fine-grained acicular ferrite, except for the self-shielded weld, where the microstructure was much coarser and the predominant microstructural constituent was FS(A). This coarse microstructure is considered to be largely a consequence of the low inclusion content of this deposit.

3) A stress relief heat treatment produced a complex pattern of mechanical property changes in which strength was normally reduced, although deposit strength still always exceeded the requirements of the base plate. In both the first side root and the second side subsurface regions, hardness was reduced.

4) In the groove welds that were produced, all consumables gave as-welded weld metal Charpy V-notch toughness exceeding that required for the plate (≥27 J at –50°C), except for the root region of the self-shielded deposit. The Charpy toughness changes produced by a stress relief heat treatment did not follow a consistent pattern. In many cases, toughness was reduced at the lower energy levels (27 J), but for several of the welds the toughness was increased at higher levels (100 J). The rutile flux cored deposit suffered severe degradation of toughness during stress relieving, with the Charpy transition curve being shifted to higher temperatures by ≥~60°C.

5) The as-welded critical CTOD data indicated that the welds were fit for service over a wide range of temperatures. The lowest temperatures at which upper shelf behavior was observed were –30°C for the basic flux cored deposit, –10°C for the rutile flux cored deposit, and 10°C for the self-shielded flux cored deposit and the metal cored deposit. The toughness of the solid welding wire deposit was only marginally lower than that of the rutile flux cored deposit. The critical CTOD of the welds was generally improved substantially by a stress relief heat treatment. The exception to this was the rutile flux cored wire weld, where a substantial reduction in toughness occurred once again, with a change from upper shelf to lower shelf behavior at –10°C.

6) The substantial reduction in toughness that occurred in the rutile flux cored weld upon stress relief heat treatment is attributable to a change in fracture mode, at least in the as-deposited and grain-coarsened reheated regions, from ductile to intergranular fracture.

Acknowledgments

Assistance with the experimental work provided by colleagues at The Welding Institute, particularly S. A. W. Sleep, C. S. Hunt, K. W. Middleton, J. C. Ford, P. S. Touhey, S. E. Courtney, S. M. Stevens, W. Martin, P. Rodwell and G. Baldacchino, is gratefully acknowledged, as are helpful discussions with R. L. Jones, C. S. Hunt, N. Bailey, T. G. Gooch and P. H. M. Hart.

The work was funded jointly by Research Members of The Welding Institute and by the Minerals and Metals Division of the U.K. Department of Trade and Industry.

References

1. Smith, D. C. 1970. *Welding Journal* 49(7):535–547.

2. Jones, R. L. 1980. The flux cored arc welding of carbon manganese steels — a review of the present position. Welding Institute Members Report 125/1980.

3. George, M. J., Still, J. R., and Terry, P. 1981. *Met. Con.* 13 (12):730–737.

4. Keeler, T. 1981. *Met. Con.* 13(11):667–673 and 13(12):750–753.

5. Jones, R. L. 1986. Properties of welds made by the flux cored arc welding process. Presented at Welding Institute Workshop, Aberdeen. (Based on Ref. 6.)

6. Jones, R. L., and Pisarski, H. G. 1984. A study of the mechanical properties of flux cored wire welds in C-Mn steels. Welding Institute Members Report 241/1984.

7. Amin, M., and Watkins, P. V. C. 1977. Synergic pulsed MIG welding. Welding Institute Members Report 46/1977/P.

8. Rogers, P. 1985. *Met. Con.* 17(9):602–604.

9. Wiseman, R. 1984. Pulsed MIG: a new era in MIG welding. *Welding News* (186):12, 13.

10. Brosilow, R. 1984. *Welding Design and Fabrication* 57(10):57–68, 70.

11. Ma, J. and Apps, R. L. 1983. *Weld and Met Fab* 51(4) 168–170, 172–175.

12. Allum, C. J. 1986. Recent developments in pulsed gas metal arc welding. Proc. Conf. on Welding for Challenging Environments. pp. 1–10. The Welding Institute of Canada, Pergamon, Toronto, Canada

13. Blackman, S. A. 1986. The use of pulsed MIG welding parameters with flux cored wires. The Welding Institute Seminar on Exploiting Developments in MIG and Flux-Cored Wire Welding, Bradford, England.

14. Norris, J., Hilton, D. E., and Mistry, H. R. 1986. The effect of shielding gas composition in the MAG welding of line pipe. Proc. Conf. on Welding and Performance of Pipelines, Paper 19, The Welding Institute, Abington, London, England.

15. Dorling, D. V., Huntley, R. M., and Rothwell, A. B. 1986. All-position mechanized and automated FCAW systems for the fabrication of offshore structures and arctic vessels. Proc. Conf. on Welding for Challenging Environments, pp. 51–64, The Welding Institute of Canada, Pergamon Press, Toronto, Canada.

16. Street, J. A. 1984. Portable printing arc welding monitor aids procedure set-up and QA. Weld. Inst. Res. Bull. 25(1):14–17.

17. Pisarski, H. G., and Dawes, M. G. 1980. Measurement of crack opening displacement with particular reference to offshore structures. Welding Institute Members Report 111/1980.

18. Duncan, A. 1987. Guide to examination of ferritic steel weld metals. IIW Doc. IXJ-123-87.

19. Harrison, P. L., Abson, D. J., Jones, A. R., and Sparkes, D. J. 1989. Fractographic and metallographic study of the initiation of brittle fracture in weldments. Quantitative Methods in Fractography, ASTM STP 1085, 1990, 102-122.

20. Bailey, N., and Pargeter, R. J. 1978. The influence of flux type on the strength and fracture toughness of mild steel weld metal. Part 1: Two-pass welds. Welding Institute Members Report 70/1978/M.

21. Roberts, W., Ahlblom, B., and Hannerz N-E. 1982. Relationship between inclusion size distribution and Charpy V upper-shelf energy for structural steel weld metal. Advances in the Physical Metallurgy and Applications of Steels, pp. 162–168, , including the discussion to Session 2, The Metals Society, Also, IIW Doc.II-A-540-81, 1981.

22. Bailey, N., and Pargeter, R. J. 1979. The influence of flux type on the strength and fracture toughness of mild steel weld metal, Part 2: multipass welds. The Welding Insti-

tute Members Report 100/1979.

23. Baryshev, V. M., Shebaron, A., Birbrover, A. N., and Nalov, V. V. 1978. Increasing the cold resistance of weld metal in the multipass submerged-arc welding of a low alloy steel of type 16GZAF. *Weld. Prod.* 25(7):43–45.

24. Tweed, J. H., and Knott, J. F. 1983. Metal Science 17(2): 45–54.

25. Tweed, J. H., and Knott, J. F. 1982. Microstructure-toughness relationships in a C-Mn weld metal. Proc. of 4th European Conf. on Fracture (EGF-4), Materials Advisory Services Ltd., K. L. Maurer, and F. E Matzer, (ed), pp. 127–133.

26. Terlinde, G., Muller, L., Beaven, P. A., and Schwalbe, K-H. 1984. Microstructural effects on the toughness of FCAW-ferritic weld metal. Proc. 5th European Conf. on Fracture (ECF-5), Sociedade Portuguesa de Materials, Seccao, Techica Fractura, Lisbon, Portugal, L. Faria (ed), pp. 257–268.

27. Shiliang, W., Weiping, H., and Bogang, T. 1987. *Weld. Intl.* 1(3):284–287. (Translation from Trans. China Weld. Inst., 1986, 7(2):56–63.)

28. Chen, J. H., and Van, C. 198B. The fracture behavior of C-Mn steel multipass MMA weld metals at –6°C in Charpy V testing. *Materials Science and Technology* 4(8):732–739.

29. Abson, D. J. 19B6. The influence of manganese and coating basicity on the microstructure and mechanical properties of vertical-up MMA welds in 38mm thick C-Mn-Nb steel plate — final report. Welding Institute Members Report 309/1986.

30. Garland, J. G., and Kirkwood, P. R. 1976. Metallurgical factors controlling weld metal toughness in the seam welding of line pipe. Paper presented at the AWS Annual Meeting, Atlanta, Ga., and published in *Welding of Line-Pipe Steels*, D. E. Osbourne, (ed), Welding Research Council, 1977, pp. 176–227.

31. Taylor, D. J., and Evans, G. M. 1983. Development of MMA electrodes for offshore fabrication, *Met. Con.* 15(8):438–443.

32. Anderson, T. L. 1984. Effect of crack tip region constraint on fracture in the ductile-to-brittle transition. National Bureau of Standards Report NBSIR 84-3001, Boulder, Co.

33. Towers, O. L., and Carwood, S. J. 1981. The use of maximum load toughness for ductile fracture assessments. Welding Institute Members Report 157/1981.